

This discussion paper is/has been under review for the journal Hydrology and Earth System Sciences (HESS). Please refer to the corresponding final paper in HESS if available.

Transient analysis of fluctuations of electrical conductivity as tracer in the streambed

C. Schmidt, A. Musolff, N. Trauth, M. Vieweg, and J. H. Fleckenstein

Department Hydrogeology, Helmholtz Centre for Environmental Research – UFZ,
Permoserstrasse 15, 04318 Leipzig, Germany

Received: 27 April 2012 – Accepted: 5 May 2012 – Published: 23 May 2012

Correspondence to: C. Schmidt (christian.schmidt@ufz.de)

Published by Copernicus Publications on behalf of the European Geosciences Union.

HESSD

9, 6345–6365, 2012

Transient analysis of fluctuations of electrical conductivity

C. Schmidt et al.

Title Page

Abstract

Introduction

Conclusions

References

Tables

Figures

⏪

⏩

◀

▶

Back

Close

Full Screen / Esc

Printer-friendly Version

Interactive Discussion

Abstract

Magnitudes and directions of water flux in the streambed are controlled by hydraulic gradients between the groundwater and the stream and by bedform-induced hyporheic exchange flows. These water fluxes vary over time driven by for instance by short term flood events or seasonal variations in stream flow and groundwater level. Variations of electrical conductivity (EC) are used as a natural tracer to detect transient travel times and flow velocities in an in-stream-gravel bar. We present a method to estimate travel times between the stream and measuring locations in the gravel bar by non-linearly matching the EC signals in the time domain. The amount of temporal distortion required to obtain the optimal matching is related to the travel time of the signal. Our analysis revealed that the travel-times increased at higher stream flows because lateral head gradients across the gravel bar are leveled at the time.

1 Introduction

The interface between streams and groundwater has long been recognized as an important reactive zone for coupled stream-groundwater systems (e.g. Triska et al., 1993; Findlay, 1995). Typically, steep biogeochemical gradients occur as a result of the direction and magnitude of water fluxes and the reaction kinetics (Geist and Auerswald, 2007; Boano et al., 2010; Schmidt et al., 2011). Understanding water flow and solute transport at the stream-groundwater interface requires elucidating both, spatial patterns and temporal dynamics of flow paths and travel times. Spatial pattern of water fluxes are caused by the heterogeneity of streambed sediments and the resulting hydraulic conductivity, streambed and stream morphology as well as the spatial connectivity to the groundwater. Temporal variations of flow are a result of varying hydraulic conditions in both the stream and the aquifer. Changes of magnitude and direction flow in the streambed can be induced by flood events (e.g. Vogt et al., 2010a) by seasonal variations of flow systems (Wroblicky et al., 1998) or by rising groundwater levels

HESSD

9, 6345–6365, 2012

Transient analysis of fluctuations of electrical conductivity

C. Schmidt et al.

Title Page

Abstract

Introduction

Conclusions

References

Tables

Figures

⏪

⏩

◀

▶

Back

Close

Full Screen / Esc

Printer-friendly Version

Interactive Discussion



caused by increased recharge (Schmidt et al., 2011) or combinations of various factors (Käser et al., 2009). Quasi-regular variations of hydraulic conditions may be induced by dam operation (Sawyer et al., 2009), tidally influenced streams (Westbrook et al., 2005; Bianchin et al., 2010) or diurnal groundwater level variation induced by evapotranspiration of riparian vegetation (Valett, 1993). Lateral hydraulic gradients can exist between branching channels. The lateral flow through islands and bars varies with changing water levels in the individual channels (Wondzell and Gooseff, 2012).

Detecting temporal variations of hydraulic conditions and water flow in the field requires measurements at a time interval shorter than that of the temporal variation of interest. Sensors and data loggers for monitoring of physical parameters such as water level, temperature and electrical conductivity (EC) are commercially available and allow a simple collection of highly resolved time series data for groundwater surface water studies.

Time-series of hydraulic heads and the subsequent calculation of hydraulic gradients may not be a good indicator of flow. Heads in the streambed may increase proportionally to the water level in the stream reflecting the hydraulic connection and the pressure propagation but not the magnitude and direction of flow (Käser et al., 2009; Vogt et al., 2010b).

Natural fluctuations of water temperature and EC can be used as a tracer for flow in the streambed and thus providing a direct estimate of travel times. The use of heat as tracer has steadily increased in recent years and has practically become the standard natural tracer for ground-water surface water interaction studies. Particularly, diurnal temperature variations in the surface water provide a convenient, periodic signal that can be easily extracted and evaluated for the advective heat flow component and thus for vertical water flux (Keery et al., 2007; Hatch et al., 2006; Rau et al., 2012; Vogt et al., 2010a; Schmidt et al., 2011). Heat tracing methods have recently been advanced by vertical high resolution fibre-optic distributed temperature sensors allowing to determining spatial and temporal variations of vertical water fluxes (Briggs et al., 2012; Vogt et al., 2010a). Besides temperature, EC of stream water also fluctuates driven by

Transient analysis of fluctuations of electrical conductivity

C. Schmidt et al.

Title Page

Abstract

Introduction

Conclusions

References

Tables

Figures



Back

Close

Full Screen / Esc

Printer-friendly Version

Interactive Discussion

variations in temperature, stream flow and anthropogenic inputs (Cirpka et al., 2007; Vogt et al., 2010b). In contrast to the diurnal temperature signal, which is strongly attenuated in the shallow sediment, fluctuations of EC propagate deeper since EC is practically a conservative tracer. Despite this advantage however, only a few studies have analyzed EC time series (Cirpka et al., 2007; Vogt et al., 2010b; Sheets et al., 2002). Possible reasons for that could be that not all streams show sufficient EC fluctuations and that devices for logging EC-time series are comparably more expensive than standard temperature sensors.

Travel times can be generally inferred from continuous natural tracers by estimating the time lags between the input and the output signals. The time lag between two continuous signals can be regarded as the dominant advective travel time of the tracer. This would be equal to the timing of the peak breakthrough of a tracer pulse. Assuming a stationary process, the characteristic time lag can be easily estimated by cross-correlation (Sheets et al., 2002; Vogt et al., 2010b). More sophisticated, deconvolution provides a transfer function that characterizes the time lag and the impulse response of the system (Cirpka et al., 2007; Vogt et al., 2010b). It is assumed that the EC time series in the streambed is a response to the EC input series in the stream. Since we expect variable flow conditions in the streambed (e.g. Lewandowski et al., 2011), the assumption of stationarity does not hold. Thus, a transient method is needed. In their analysis Vogt et al. (2010a) have shown that dynamic harmonic regression (DHR) can be used to derive transient time lags from temperature time series. However, DHR requires periodic signals which are not necessarily found for EC in streams.

Windowed cross correlation may be used to capture transient time lags. The basic idea is to slide overlapping subsequences of a certain length (the window) to construct a matrix with correlation coefficients with time indices versus time lags (Boker et al., 2002). However, the analysis by Boker et al. (2002) was limited to visual inspection of the correlation matrix. What is required is an extraction of the optimal time lag over time. We propose to apply a Dynamic Time Warping (DTW) algorithm to estimate variable time lags. DTW has long been used for speech recognition (e.g. Sakoe and Chiba,

Transient analysis of fluctuations of electrical conductivity

C. Schmidt et al.

Title Page

Abstract

Introduction

Conclusions

References

Tables

Figures



Back

Close

Full Screen / Esc

Printer-friendly Version

Interactive Discussion

1978), where the sound signals of different speakers often exhibit speed and acceleration shifts. DTW performs an element by element alignment. Thus, rather than just shifting a time series along the time axis it allows non-linear “shrinking” and “extending” which is summarized by the term “warping”. The time lag between two time series can be inferred from the amount of “warping” required to obtain the optimal fit. In this study, we introduce a modified, windowed DTW approach to evaluate the variability of advective travel times between the stream and the streambed based on time series of EC.

2 Theory

2.1 Fluctuations of electrical conductivity

Natural tracers that can be easily recorded with automated data loggers are a suitable means to study transient flow processes. Tracing diurnal temperature variations has become a well-established method for assessing stream-groundwater exchange. However, diurnal temperature signals are often strongly attenuated in sediments as conductive heat exchange with the matrix of the porous medium can result in significant damping of the signal.

In contrast EC, a parameter representing the concentration of solute ions in the water, shows much less attenuation. EC in streams also exhibits fluctuations that can be used as tracer similarly to temperature variations (Vogt et al., 2010b). A variety of factors influences EC fluctuations in streams. Increasing discharge resulting from rains events is associated with decreasing EC due to a diluting effect of the rain water. Conversely, evapotranspiration can result in an increase of EC and a decrease of discharge (Calles, 1982). Changes of groundwater discharge may also influence EC in the stream since groundwater has typically higher EC values. The uptake of CO₂ by primary production causes a reduction of bicarbonate and this may cause a reduction of EC, typically at diurnal temperature maxima (Ort and Siegrist, 2009). Effluents from

Transient analysis of fluctuations of electrical conductivity

C. Schmidt et al.

Title Page

Abstract

Introduction

Conclusions

References

Tables

Figures



Back

Close

Full Screen / Esc

Printer-friendly Version

Interactive Discussion



wastewater treatment plants (WWTP) typically increase stream EC values. Effluent discharges are higher during the day and have thus an increasing effect on EC during day times. Dam operations can also influence downstream EC since the released water can have a different EC signature. Fluctuations of EC at our study location show the diluting effect of rain events. Intraday fluctuations of EC coincident with fluctuations of stream flow, induced by the operation of a water mill located upstream of the site. Generally, the mill-driven discharge peaks decrease stream water EC at our site.

2.2 Dynamic time warping

Given two discrete time series A and B of length n and m with $A = a_1, a_2, \dots, a_i, \dots, a_n$ and $B = b_1, b_2, \dots, b_j, \dots, b_m$, we can build a n by m distance matrix where each element (i, j) contains the pairwise squared distances $\mathbf{d}(a_i, b_j) = \text{sqrt}(a_i - b_j)^2$. An alignment between A and B can be found by minimizing the cumulative distance $D(i, j)$ between the current element $\mathbf{d}(a_i, b_j)$ and the adjacent elements in the distance matrix starting at $\mathbf{d}(a_1, b_1)$ and ending at $\mathbf{d}(a_n, b_m)$. In other words, the algorithm finds the minimum cost path through the distance matrix. The minimum cost path aligns (warps) the time axis of the two series. The recursive algorithm to find the minimum cost path through a distance matrix is given by (e.g. Sakoe and Chiba, 1978):

$$D(i, j) = \mathbf{d}(a_i, b_j) + \min \{D(i - 1, j - 1), D(i - 1, j), D(i, j - 1)\} \quad (1)$$

Once the minimum cost path through the cumulative distance matrix has been determined, the time lag for each element of A and B can be obtained from the shift of the minimum cost path from unity. Equal or non-time shifted time series would result in a minimum cost path through the distance matrix exactly on the diagonal of the matrix. Whenever a time lag exists, the minimum cost path will deviate from the diagonal. Hence, for each element of A there is a time lag τ that minimizes the distance measure.

For our example we can constrain the minimum cost path $p(i, j)$ to be continuous so that i and j maximally increase by one at each step along the path and to be monotonic

Transient analysis of fluctuations of electrical conductivity

C. Schmidt et al.

Title Page

Abstract

Introduction

Conclusions

References

Tables

Figures

⏪

⏩

◀

▶

Back

Close

Full Screen / Esc

Printer-friendly Version

Interactive Discussion



so i and j can only increase or stay the same. We can further constrain $\rho(i, j)$ to be located at one side of the diagonal of the distance matrix since the EC signal cannot be observed in the streambed before it occurred in the stream ($\rho(j) \geq \rho(i)$). Figure 1a shows two time series where the black line represents the input series and the blue line depicts the lagged response. It can be seen that the time lag steadily decreases with time. In Fig. 1b the resulting distance matrix with the minimum cost path is visualized. The distance between identity (diagonal through the distance matrix) and the minimum cost path decreases with time in accordance with the decreasing time lag between the two signals in Fig. 1a.

2.3 Dynamic time warping with sliding window

The element by element alignment of two measured time series with data containing noise may result in noisy, non-smooth minimum cost paths. Local differences of amplitudes may lead to artificial warping paths with singularities, where a single point in time of one time series is mapped onto a subsection of the other time series (Keogh and Pazzani, 2001). To avoid noisy warping paths with singularities we modified the original DTW approach. We create a distance matrix in which each element represents the distance between two sub-series of A and B defined by the window length rather than creating a pairwise distance matrix.

$$d(a_i, b_j) = \text{dist}(a_i \dots a_{i+1} \dots a_{i+w}, b_j \dots b_{j+1} \dots b_{j+w}) \quad (2)$$

where w is the length of the sliding window given by the number of discrete elements and dist is a distance measure which is not necessarily the Euclidean distance. The windowed distance matrix will be cut at the edges at a value equal to the time series length minus by the window length $i_{\max} = n - w$, $j_{\max} = m - w$.

The window length should be selected in a way that it contains a sufficient number of “features” of the time series to ensure a clear minimum in the function for the distance measure at perfect alignment. For example to align two sinusoidal signals we recommend to use a sliding window not short than the semi-period of the signal.

Transient analysis of fluctuations of electrical conductivity

C. Schmidt et al.

Title Page

Abstract

Introduction

Conclusions

References

Tables

Figures

⏪

⏩

◀

▶

Back

Close

Full Screen / Esc

Printer-friendly Version

Interactive Discussion



Euclidean distance is the common distance measure for DTW and other optimization and classification applications. However, Euclidean distance does not provide a standardized measure for the goodness of fit. A distance matrix based on correlation coefficients is a good alternative. Instead of calculating the Euclidean distance between the subsequences of length w of the signal, we use the Pearson sample correlation coefficient. By using the correlation coefficient we can easily obtain information on how good the two subsequences actually match when they are optimally aligned.

$$\mathbf{d}(a_i, b_j)_r = \frac{w \sum_{k=i}^{i+w} a_k b_k - \sum_{k=i}^{i+w} a_k \sum_{k=i}^{i+w} b_k}{\sqrt{w \sum_{k=i}^{i+w} a_k^2 - \left(\sum_{k=i}^{i+w} a_k \right)^2} \sqrt{w \sum_{k=i}^{i+w} b_k^2 - \left(\sum_{k=i}^{i+w} b_k \right)^2}} \quad (3)$$

Instead of finding the minimum cost path, searching the optimal path through a correlation matrix requires maximizing the cumulative distance which represents the sum of the correlation coefficients along the path. The maximum correlation path (MCP) for correlation coefficients ranging from -1 to 1 can be easily found by minimizing the cost path through the correlation matrix containing elements calculated by:

$$\mathbf{d}(a_i, b_j)_{\text{MCP}} = 1 - \mathbf{d}(a_i, b_j)_r \quad (4)$$

Where d_{MCP} is the distance measure to be used by the algorithm given in Eq. (1).

3 Study site and experimental setup

3.1 Study site

The study site is located in an alluvial floodplain at a reach of the Selke River characterized by pronounced meanders, pool riffle sequences and point and mid-channel

Transient analysis of fluctuations of electrical conductivity

C. Schmidt et al.

Title Page

Abstract

Introduction

Conclusions

References

Tables

Figures

⏪

⏩

◀

▶

Back

Close

Full Screen / Esc

Printer-friendly Version

Interactive Discussion



bars (Fig. 2a). The catchment of the Selke River drains an area of 458 km², the long-term mean discharge is 1.5 m³ s⁻¹. The alluvial aquifer is 5 to 6 m thick and consists of interbedded sands and gravels that are underlain by less permeable triassic lime and sand stone. The gravel streambed has hydraulic conductivities ranging from 2.7 × 10⁻⁴ to 6.0 × 10⁻³ ms⁻¹, which were determined by falling head slug tests. For a detailed description of the slug test method see Schmidt et al. (2006). The hydraulic gradients between the stream and the groundwater have been found to alternate seasonally based on stream water level data and head measurements in adjacent groundwater monitoring wells. The in-stream-gravel bar is characterized by visually observable lateral hydraulic gradients between the main and the side channel (Fig. 2b). The differences in water level arise from the steeper slope of the side channel at the upstream end of the gravel bar. As the stream flow increases this morphologic effect levels off.

3.2 Experimental setup and data collection

Self-contained EC, pressure and temperature sensors with data loggers (Solinst 3001 LTC Levellogger Junior) were deployed in the stream and at two locations in the streambed at the upstream (Upstream Streambed Sensor, USS) and downstream (Downstream Streambed Sensor, DSS) end of an in stream gravel bar (Fig. 2a). To install the streambed loggers a screened steel tube with drive point was driven into the streambed. The EC sensor is placed inside the tube exactly at the 2 cm long screen at the bottom of the device. Unlike with a piezometer, the top of the tube is at level with the streambed surface and does not rise into the water column to avoid any surface flow obstruction. After the logger deployment the tube is closed with a threaded lid at the top to ensure that the pressure measurements are not affected by hydrostatic pressure when the device is submerged. The centre of the screen of each tube is located at a depth of 0.44 m below the streambed surface. The accuracies of the sensors as reported by the manufacturer are 1 cm for pressure, 0.1 °C for temperature and 20 μS cm⁻¹ for EC. Measured EC values are internally compensated for temperature to

Transient analysis of fluctuations of electrical conductivity

C. Schmidt et al.

Title Page

Abstract

Introduction

Conclusions

References

Tables

Figures



Back

Close

Full Screen / Esc

Printer-friendly Version

Interactive Discussion



derive specific electrical conductivities. Data was recorded at a 10 min interval between 13 July and 2 September 2011.

4 Results

4.1 Time series data

Figure 3a shows the water level in the stream and the total hydraulic head recorded in the streambed (normalized to the streambed surface at the USS and DSS location). Generally, during the data collection period in summer 2011 losing conditions were prevalent. However, the flood pulse around the 25 August apparently diminishes the hydraulic head differences. Superimposed onto the general water level are short term pulse-like fluctuations, which increase the water level by 5 to 10 cm. These peaks are due to mill operations upstream of the study site.

The general pattern of EC inversely follows the water level for rain events. High water level and thus stream flow is associated with lower EC due to a dilution effect of rain water. The mill-induced, pulse-like water level fluctuations also decrease the EC but not to the same extent as rain events. The mean EC is lowest in the stream with $576 \mu\text{Scm}^{-1}$. In the streambed the mean EC is $588 \mu\text{Scm}^{-1}$ at the USS and $601 \mu\text{Scm}^{-1}$ at the DSS location, respectively. These values are similar to observed EC values measured manually in observation wells located close to the stream banks. EC of groundwater that is potentially not influenced by the stream is around 1020 to $1170 \mu\text{Scm}^{-1}$ manually measured in two wells located approximately 160 m and 500 m away from the left and right river banks, respectively. Variations of EC in the stream range between 354 and $694 \mu\text{Scm}^{-1}$. The lowest value was observed during the flood event and interpreted as a dilution effect. The EC variation in the stream has an approximate mean period of 16 h. The mean period was estimated based on the number of zero crossings of the entire EC signal (normalized to zero mean). The mean EC amplitude in the stream during one period is $21 \mu\text{Scm}^{-1}$. The EC signal in the streambed lags the stream signal at

Transient analysis of fluctuations of electrical conductivity

C. Schmidt et al.

Title Page

Abstract

Introduction

Conclusions

References

Tables

Figures



Back

Close

Full Screen / Esc

Printer-friendly Version

Interactive Discussion



both the USS and DSS location. The time lags between the stream and the streambed sensors change over time. As illustrated in Fig. 4a between 17 July and 19 July the DSS response occurs later than the one at the USS. Between 18 August and 20 August for example the USS response occurs before the DSS response (Fig. 4b). The characteristic features and amplitudes in all time series are similar indicating no general dampening or smearing of the signal. This indicates short flow paths. However, high frequency components in the stream EC are partially damped and do not occur in the streambed indicating some damping (Fig. 4c).

4.2 Time lags

Overall the time lags are short. Figure 5 shows the estimates of the characteristic transient time lags for the USS and DSS and the underlying correlation matrix $d(a_i, b_j)_r$ rotated by 45° to map the diagonal on the x-axis. The mean time lags of both streambed sensors are similar with 2 h 21 min for the USS and 2 h 54 min for the DSS, respectively. However, the DSS is characterized by a shorter mode of 1 h 40 min while the mode of the USS is 2 h 20 min. At the downstream location a wider range of time lags was observed than at the USS location. (Standard deviations: USS 56 min, DSS 2 h 29 min.) For comparison, cross-correlation analysis reveals a time lag of 2 h for the USS and 1 h 40 min for the DSS. These values are exactly (1 h 40 min) and close to (2 h 20 min) the modes of the transient time lag.

During and after the flood event between 24 and 25 August occur the highest differences of the estimated time lags. Clearly, the USS shows a different response to the flood event. The time lag remains relatively unaffected. This is in accordance with the hydraulic gradient. At the peak of the flood event the hydraulic head difference almost reached zero at the DSS location, while at the USS a smaller but still losing gradient was observed. Accordingly, at the DSS location the time lag quickly increases during the flood pulse from less than 2 h to 11 h and remains high for the rest of the analyzed time span. Thus, the USS and DSS locations have a different response to flood pulse for both, the hydraulic gradient and the EC – based characteristic time lag.

Transient analysis of fluctuations of electrical conductivity

C. Schmidt et al.

Title Page

Abstract

Introduction

Conclusions

References

Tables

Figures



Back

Close

Full Screen / Esc

Printer-friendly Version

Interactive Discussion



Transient analysis of fluctuations of electrical conductivity

C. Schmidt et al.

Title Page

Abstract

Introduction

Conclusions

References

Tables

Figures

⏪

⏩

◀

▶

Back

Close

Full Screen / Esc

Printer-friendly Version

Interactive Discussion



The similar time lags between the stream and both, the USS and DSS, suggest similar flow path lengths from the stream to the sensors. Longer hyporheic flow paths resulting from downwelling of stream water at the upstream side of the gravel bar (at the USS) and reemergence at the downstream end (at the DSS) would have caused an observable dampening of the signal and a longer time shift at the DSS.

The correlation matrices optically reveal the band of high correlation that encloses the optimal MCP (Fig. 5a, b). In general, there is an excellent correlation of the EC time series along the (MCP) whose correlations coefficients (r_{MCP}) have a mean of 0.80 at the downstream and 0.87 at the USS. Median values of 0.84 and 0.91 indicate that the distribution is slightly skewed towards higher r_{MCP} .

For both sensors vertical bands of high correlation occur. These high correlation bands have a similar timing and shape for both sensors. They are a result of low amplitudes in the stream EC signal. An extreme case would be a constant signal with no variations. This would result in a correlation coefficient of 1 when two constant subsequences are sliding along each other. The confidence intervals of the correlation coefficient were estimated applying Fisher transformation. The confidence interval varies over time and so does the range of plausible time lags. Wide confidence bounds occur when the correlation coefficients are similar for a wide range of time lags. For example, both sensors show relatively low correlation coefficients (~ 0.2 – ~ 0.6) between 25–27 July for all time lags and hence a high uncertainty of the time lag estimate. Wide confidence bounds also occur when moderate correlation coefficients (~ 0.5 – ~ 0.75) occur over a wide range of time lags as for instance at the downstream sensor at 14 August and after the flood event.

5 Discussion and conclusion

The time lag of the EC signal between the stream and the streambed sensor can be interpreted as the advective travel time of water. Thus, the vertical component of the total flow vector in the streambed can be easily estimated from the time lag and the

depths of the sensors. At the USS and DSS the mean apparent vertical flow velocities are 5.4 m d^{-1} with a standard deviation of 2.6 m d^{-1} and 6.3 m d^{-1} (standard deviation: 5.3 m d^{-1}), respectively.

The vertical water flux was estimated from the product of the vertical hydraulic gradients obtained from the pressure time series and the hydraulic conductivity determined from slug tests. Average horizontal hydraulic conductivity was determined to be at $4 \times 10^{-4} \text{ m s}^{-1}$. Assuming a horizontal to vertical anisotropy ratio of 3 and an effective porosity of 0.3, the mean advective vertical flow velocity estimated from Darcy's law is 7.9 m d^{-1} (standard deviation: 4.8 m d^{-1}) at the USS and 7.3 m d^{-1} (standard deviation: 5.0 m d^{-1}) at the DSS location. Since both estimates reasonably agree, the water flux at both sensor locations is likely to have a strong vertical component. This is in general agreement with the losing observed during the monitoring period. The hydraulic gradient between the main and the side channel potentially also contributes to the vertical flux component during low flow conditions. However, the anisotropy and porosity of the sediments are unknown. Thus, a higher anisotropy or higher porosity would result in lower Darcy-based vertical flow velocities. In turn, this would indicate a longer, non-vertical flow path of the EC-signal.

Vertical hydraulic gradients may not provide a good indication for direction and magnitude of water flow particularly under variable hydrologic conditions (Käser et al., 2009). Apart from the good match during the flood event, hydraulic head differences and EC time lag are not always consistent. Some uncertainty arises from the stream water level data during very low flows, where the depth of the water column is close to the limit of the applicability of the pressure sensor. However, there are other observations that cannot be attributed to measurement errors. For instance there is no indication in the hydraulic data for the relatively high time lag at the downstream sensor at the beginning of the observation period. Moreover, the extremely short time lag on 24 August can also not be explained from the hydraulic head difference at this time.

We have estimated the transient advective travel times between the stream and two locations the streambed based on dynamic time warping of EC time-series. The original

Transient analysis of fluctuations of electrical conductivity

C. Schmidt et al.

Title Page

Abstract

Introduction

Conclusions

References

Tables

Figures

⏪

⏩

◀

▶

Back

Close

Full Screen / Esc

Printer-friendly Version

Interactive Discussion

DTW-approach is prone to noisy estimates of travel times. The DTW algorithm may also produce singularities. To avoid noise and singularities the standard DTW algorithm was modified by applying a sliding window to ensure smooth and unique travel time variations. The method generally provides robust results when no pronounced damping of the output signal by diffusion and dispersion occurs. The characteristic shape of the input and out signal should be nearly the same as it is in our case. However, similarly to cross-correlation analysis a filter can be applied to the input series in order to obtain a similar degree of smoothness for both time series.

The correlation matrix shown in Fig. 5 provides additional information on how close the streambed EC is related to the stream water EC. Low correlation coefficients for any time lag may indicate relevant dispersive and diffusive processes during transport through the streambed or simply a sensor failure. Low correlation coefficients are associated with high uncertainty of the estimated time lag. High correlation coefficients over a range of possible time lags are caused by small gradual EC variations or portions of the EC time series that contain no or little fluctuations on the time scale of the sliding window length.

Our transient DTW based time series analysis can provide insights into the temporal dynamics of advective travel times in the streambeds that are not easily obtained from other methods. Using a sliding window instead of element by element warping makes the methods less sensitive to noise.

References

- Bianchin, M., Smith, L., and Beckie, R.: Quantifying hyporheic exchange in a tidal river using temperature time series, *Water Resour. Res.*, 46, W07507, doi:10.1029/2009WR008365, 2010.
- Boano, F., Demaria, A., Revelli, R., and Ridolfi, L.: Biogeochemical zonation due to intrameander hyporheic flow, *Water Resour. Res.*, 46, W02511, doi:201010.1029/2008WR007583, 2010.

Transient analysis of fluctuations of electrical conductivity

C. Schmidt et al.

Title Page

Abstract

Introduction

Conclusions

References

Tables

Figures



Back

Close

Full Screen / Esc

Printer-friendly Version

Interactive Discussion



Transient analysis of fluctuations of electrical conductivity

C. Schmidt et al.

Title Page

Abstract

Introduction

Conclusions

References

Tables

Figures

⏪

⏩

◀

▶

Back

Close

Full Screen / Esc

Printer-friendly Version

Interactive Discussion



- Boker, S., Xu, M., Rotondo, J., and King, K.: Windowed cross-correlation and peak picking for the analysis of variability in the association between behavioral time series, *Psychol. Methods*, 7, 338–355, doi:10.1037//1082-989X.7.3.338, 2002.
- Briggs, M. A., Lautz, L. K., McKenzie, J. M., Gordon, R. P., and Hare, D. K.: Using high-resolution distributed temperature sensing to quantify spatial and temporal variability in vertical hyporheic flux, *Water Resour. Res.*, 48, W02527, doi:10.1029/2011WR011227, 2012
- Cirpka, O. A., Fienen, M. N., Hofer, M., Hoehn, E., Tessarini, A., Kipfer, R., and Kitanidis, P. K.: Analyzing bank filtration by deconvoluting time series of electric conductivity, *Ground Water*, 45, 318–328, doi:10.1111/j.1745-6584.2006.00293.x, 2007.
- Findlay, S.: Importance of surface-subsurface exchange in stream ecosystems – the hyporheic zone, *Limnol. Oceanogr.*, 40, 159–164, 1995.
- Geist, J. and Auerswald, K.: Physicochemical stream bed characteristics and recruitment of the freshwater pearl mussel, *Freshwater Biol.*, 52, 2299–2316, 2007.
- Hatch, C. E., Fisher, A. T., Revenaugh, J. S., Constantz, J., and Ruehl, C.: Quantifying surface water-groundwater interactions using time series analysis of streambed thermal records: method development, *Water Resour. Res.*, 42, W10410, doi:10.1029/2005WR004787, 2006.
- Käser, D. H., Binley, A., Heathwaite, A. L., and Krause, S.: Spatio-temporal variations of hyporheic flow in a riffle-step-pool sequence, *Hydrol. Process.*, 23, 2138–2149, doi:10.1002/hyp.7317, 2009.
- Keery, J., Binley, A., Crook, N., and Smith, J. W.: Temporal and spatial variability of groundwater-surface water fluxes: Development and application of an analytical method using temperature time series, *J. Hydrol.*, 336, 1–16, 2007.
- Keogh, E. J. and Pazzani, M. J.: Derivative dynamic time warping, in: *First SIAM International Conference on Data Mining*, Chicago, IL, 5–7 April 2001, 2001.
- Lewandowski, J., Angermann, L., Nützmann, G., and Fleckenstein, J. H.: A heat pulse technique for the determination of small-scale flow directions and flow velocities in the streambed of sandbed streams, *Hydrol. Process.*, 25, 3244–3255, doi:10.1002/hyp.8062, 2011.
- Ort, C. and Siegrist, H.: Assessing wastewater dilution in small rivers with high resolution conductivity probes, *Water Sci. Technol.*, 59, 1593, doi:10.2166/wst.2009.174, 2009.
- Rau, G. C., Andersen, M. S., and Acworth, R. I.: Experimental investigation of the thermal time-series method for surface water-groundwater interactions, *Water Resour. Res.*, 48, W03530, doi:10.1029/2011WR011560, 2012.

Transient analysis of fluctuations of electrical conductivity

C. Schmidt et al.

[Title Page](#)
[Abstract](#)
[Introduction](#)
[Conclusions](#)
[References](#)
[Tables](#)
[Figures](#)
[⏪](#)
[⏩](#)
[◀](#)
[▶](#)
[Back](#)
[Close](#)
[Full Screen / Esc](#)
[Printer-friendly Version](#)
[Interactive Discussion](#)


- Sakoe, H. and Chiba, S.: Dynamic-programming algorithm optimization for spoken word recognition, *IEEE T. Acoust. Speech*, 26, 43–49, doi:10.1109/TASSP.1978.1163055, 1978.
- Sawyer, A., Cardenas, M., Bomar, A., and Mackey, M.: Impact of dam operations on hyporheic exchange in the riparian zone of a regulated river, *Hydrol. Process.*, 23, 2129–2137, 2009.
- 5 Schmidt, C., Bayer-Raich, M., and Schirmer, M.: Characterization of spatial heterogeneity of groundwater-stream water interactions using multiple depth streambed temperature measurements at the reach scale, *Hydrol. Earth Syst. Sci.*, 10, 849–859, doi:10.5194/hess-10-849-2006, 2006.
- Schmidt, C., Martienssen, M., and Kalbus, E.: Influence of water flux and redox conditions on chlorobenzene concentrations in a contaminated streambed, *Hydrol. Process.*, 25, 234–245, doi:10.1002/hyp.7839, 2011.
- 10 Sheets, R., Darner, R., and Whitteberry, B.: Lag times of bank filtration at a well field, Cincinnati, Ohio, USA, *J. Hydrol.*, 266, 162–174, doi:10.1016/S0022-1694(02)00164-6, 2002.
- Tamao Kasahara, T. and Wondzell, S. M.: Geomorphic controls on hyporheic exchange flow in mountain streams, *Water Resour. Res.*, 39, 1005–1019, doi:10.1029/2002WR001386, 2003.
- 15 Triska, F. J., Du, J. H., and Avanzino, R. J.: The role of water exchange between a stream channel and its hyporheic zone in nitrogen cycling at the terrestrial-aquatic interface, *Hydrobiologia*, 251, 167–184, 1993.
- Valett, H.: Surface-hyporheic interactions in a Sonoran Desert stream – hydrologic exchange and diel periodicity, *Hydrobiologia*, 259, 133–144, doi:10.1007/BF00006593, 1993.
- 20 Vogt, T., Schneider, P., Hahn-Woernle, L., and Cirpka, O. A.: Estimation of seepage rates in a losing stream by means of fiber-optic high-resolution vertical temperature profiling, *J. Hydrol.*, 380, 154–164, 2010a.
- Vogt, T., Hoehn, E., Schneider, P., Freund, A., Schirmer, M., and Cirpka, O. A.: Fluctuations of electrical conductivity as a natural tracer for bank filtration in a losing stream, *Adv. Water Resour.*, 33, 1296–1308, 2010b.
- 25 Westbrook, S., Rayner, J., Davis, G., Clement, T., Bjerg, P., and Fisher, S.: Interaction between shallow groundwater, saline surface water and contaminant discharge at a seasonally and tidally forced estuarine boundary, *J. Hydrol.*, 302, 255–269, 2005.
- 30 Wroblicky, G., Campana, M., Valett, H., and Dahm, C.: Seasonal variation in surface-subsurface water exchange and lateral hyporheic area of two stream-aquifer systems, *Water Resour. Res.*, 34, 317–328, 1998.

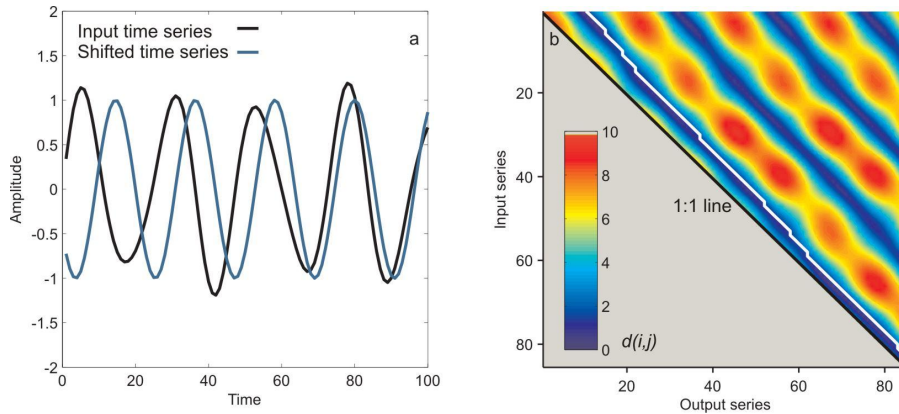


Fig. 1. (a) Example of two generic time series. The blue series decreasingly lags behind the black series. **(b)** Distance matrix of the two time series with the minimum cost path indicated

Transient analysis of fluctuations of electrical conductivity

C. Schmidt et al.

Title Page

Abstract Introduction

Conclusions References

Tables Figures

⏪ ⏩

◀ ▶

Back Close

Full Screen / Esc

Printer-friendly Version

Interactive Discussion

Transient analysis of fluctuations of electrical conductivity

C. Schmidt et al.

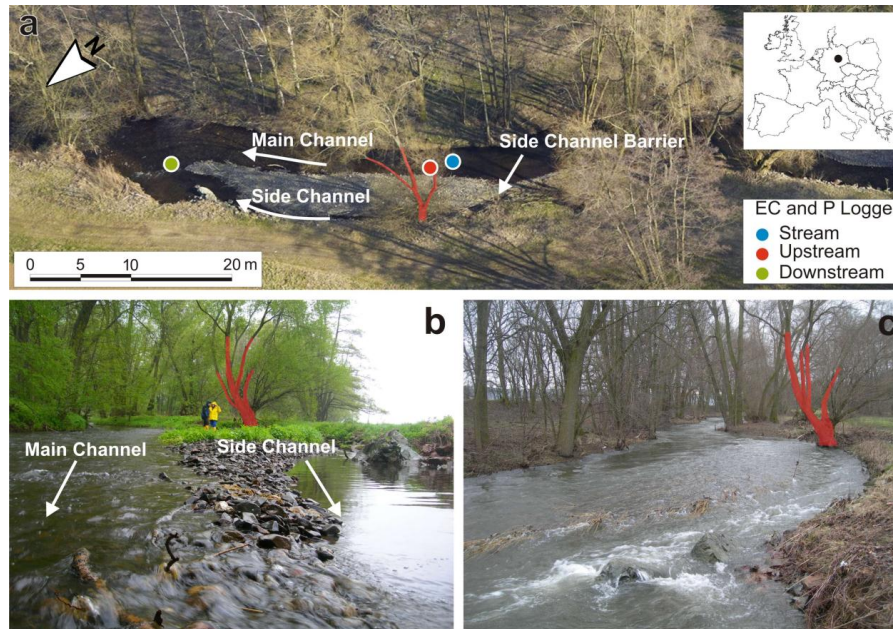


Fig. 2. (a) Aerial photograph of the studied in-stream gravel bar showing the location of the EC and pressure sensors, (b) the gravel bar during low flow (note the hydraulic gradient between the main channel and the side channel), (c) the same spot during high flow with the gravel bar submerged and the side channel fully connected. During high flow the lateral hydraulic gradients are absent. The tree marked in red is the same in each picture for better orientation.

[Title Page](#)
[Abstract](#)
[Introduction](#)
[Conclusions](#)
[References](#)
[Tables](#)
[Figures](#)
[⏪](#)
[⏩](#)
[◀](#)
[▶](#)
[Back](#)
[Close](#)
[Full Screen / Esc](#)
[Printer-friendly Version](#)
[Interactive Discussion](#)

Transient analysis of fluctuations of electrical conductivity

C. Schmidt et al.

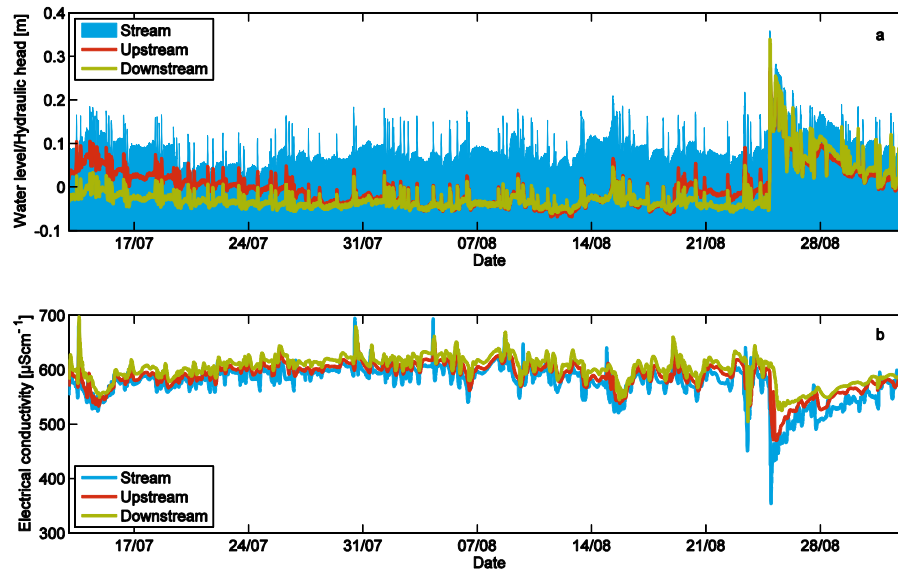


Fig. 3. (a) Time series of water level in the Selke River (blue) and hydraulic heads in the streambed at the USS and DSS location of the gravel bar. (b) Time series of electrical conductivity.

[Title Page](#)[Abstract](#)[Introduction](#)[Conclusions](#)[References](#)[Tables](#)[Figures](#)[⏪](#)[⏩](#)[◀](#)[▶](#)[Back](#)[Close](#)[Full Screen / Esc](#)[Printer-friendly Version](#)[Interactive Discussion](#)

**Transient analysis of
fluctuations of
electrical
conductivity**

C. Schmidt et al.

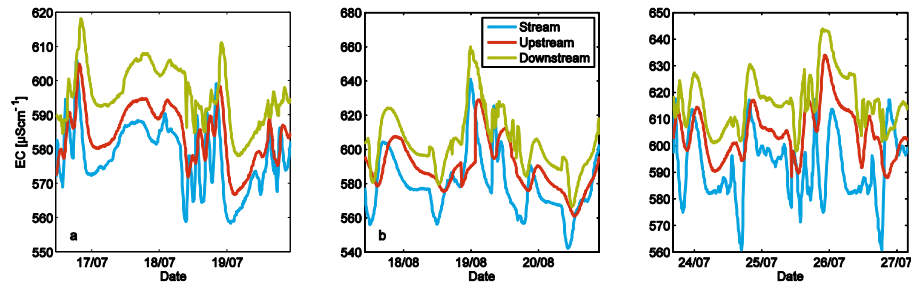


Fig. 4. Close-up of EC fluctuations for three two-day windows: **(a)** the DSS lags behind the USS, **(b)** USS lags behind the DSS, **(c)** a period with low correlation coefficients. The double peak in the stream EC signal does not propagate to the streambed sensors.

[Title Page](#)[Abstract](#)[Introduction](#)[Conclusions](#)[References](#)[Tables](#)[Figures](#)[⏪](#)[⏩](#)[◀](#)[▶](#)[Back](#)[Close](#)[Full Screen / Esc](#)[Printer-friendly Version](#)[Interactive Discussion](#)

Transient analysis of fluctuations of electrical conductivity

C. Schmidt et al.

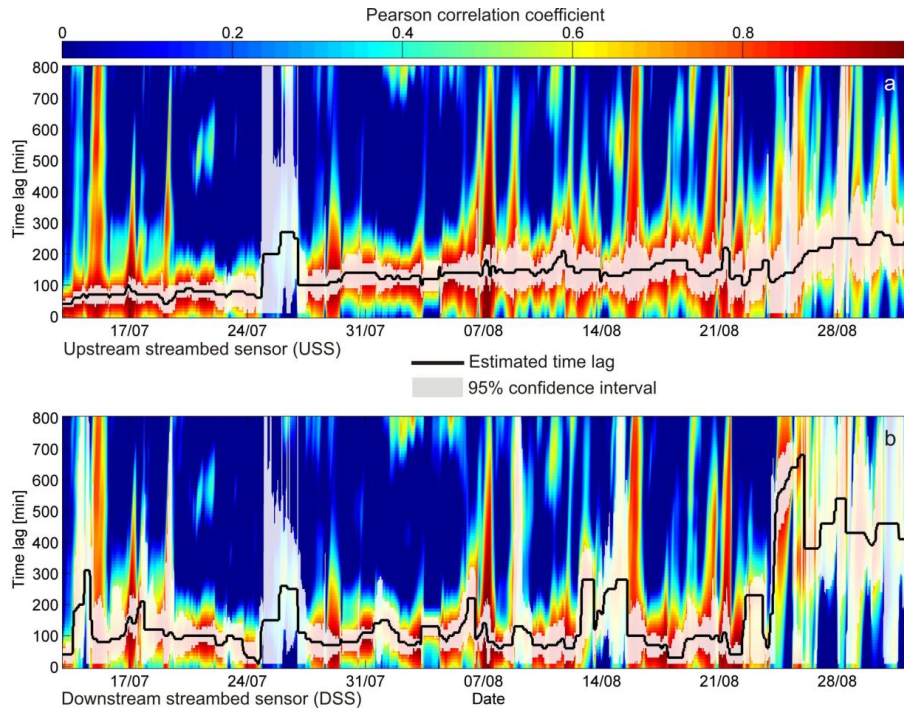


Fig. 5. Correlation matrices of the DSS and USS. Solid black line: characteristic transient time lag at the (a) USS and (b) DSS location. Shaded white area: 95% confidence interval. The data is truncated to visualize only the range of the time lags.

Title Page

Abstract

Introduction

Conclusions

References

Tables

Figures

⏪

⏩

◀

▶

Back

Close

Full Screen / Esc

Printer-friendly Version

Interactive Discussion